Since January 2020 Elsevier has created a COVID-19 resource centre with free information in English and Mandarin on the novel coronavirus COVID-19. The COVID-19 resource centre is hosted on Elsevier Connect, the company's public news and information website.

European Journal of Pharmacology 882 (2020) 173237

Contents lists available at ScienceDirect

European Journal of Pharmacology

journal homepage: www.elsevier.com/locate/ejphar

Full length article

Effective block by pirfenidone, an antifibrotic pyridone compound (5-methyl-1-phenylpyridin-2[H-1]-one), on hyperpolarization-activated cation current: An additional but distinctive target

Wei-Ting Chang[a,b,c], Eugenio Ragazzi[d], Ping-Yen Liu[a,e], Sheng-Nan Wu[f,g,h,*]

[a] Institute of Clinical Medicine, College of Medicine, National Cheng Kung University, Tainan, 70101, Taiwan
[b] Division of Cardiology, Internal Medicine, Chi-Mei Medical Center, Tainan, 71004, Taiwan
[c] Department of Biotechnology, Southern Taiwan University of Science and Technology, Tainan, 71004, Taiwan
[d] Department of Pharmaceutical and Pharmacological Sciences, University of Padova, 35131, Padova, Italy
[e] Division of Cardiology, Internal Medicine, College of Medicine, National Cheng Kung University Hospital, Tainan, 70401, Taiwan
[f] Institute of Basic Medical Sciences, National Cheng Kung University Medical College, Tainan, Taiwan
[g] Department of Physiology, National Cheng Kung University Medical College, Tainan, Taiwan
[h] Department of Medical Research, China Medical University Hospital, China Medical University, Taichung, Taiwan

ARTICLE INFO

Keywords:
Pirfenidone
Hyperpolarization-activated cation current
K^+ current
Ca^{2+} current
Voltage hysteresis
Membrane potential
Pituitary cell

ABSTRACT

Pirfenidone (PFD), a pyridone compound, is well recognized as an antifibrotic agent tailored for the treatment of idiopathic pulmonary fibrosis. Recently, through its anti-inflammatory and anti-oxidant effects, PFD based clinical trial has also been launched for the treatment of coronavirus disease (COVID-19). To what extent this drug can perturb membrane ion currents remains largely unknown. Herein, the exposure to PFD was observed to depress the amplitude of hyperpolarization-activated cation current (I_h) in combination with a considerable slowing in the activation time of the current in pituitary GH_3 cells. In the continued presence of ivabradine or zatebradine, subsequent application of PFD decreased I_h amplitude further. The presence of PFD resulted in a leftward shift in I_h activation curve without changes in the gating charge. The addition of this compound also led to a reduction in area of voltage-dependent hysteresis evoked by long-lasting inverted triangular (downsloping and upsloping) ramp pulse. Neither the amplitude of M-type nor *erg*-mediated K^+ current was altered by its presence. In whole-cell potential recordings, addition of PFD reduced the firing frequency, and this effect was accompanied by the depression in the amplitude of sag voltage elicited by hyperpolarizing current stimulus. Overall, this study highlights evidence that PFD is capable of perturbing specific ionic currents, revealing a potential additional impact on functional activities of different excitable cells.

1. Introduction

Pirfenidone (PFD, Esbriet®, 5-methyl-1-phenylpyridin-2[H-1]-one), a pyridone derivative, is thought to act by interfering with the production of transforming growth factor-β and tumor necrosis factor-α(Antoniu, 2006; Saito et al., 2019). This compound is a new anti-fibrotic drug approved by the U.S. Food and Drug Administration for idiopathic pulmonary fibrosis. Accumulating evidence has revealed the efficacy of PFD either in treating idiopathic pulmonary fibrosis (Balestro et al., 2019; Saito et al., 2019), in interstitial lung disease (Collins and Raghu, 2019), or in non-small cell lung cancer (Kanayama et al., 2020; Krämer et al., 2020). Recently, through its anti-inflammatory and anti-oxidant effects, namely by inhibiting IL-1β and IL-4, PFD has been included in a clinical trial for the treatment of *coronavirus* disease (*COVID*-19) (NCT04282902, 2020; Rosa and Santos, 2020).

In addition to its demonstrated activity in idiopathic pulmonary fibrosis, PFD has been also reported to attenuate neuronal loss and reduce lipid peroxidation in the pubescent rat hippocampus (Castro-Torres et al., 2014), as well as to diminish cerebral ischemia-reperfusion injury (Peng et al., 2019). Moreover, in cardiac myocytes, PFD has been shown to influence increased the amplitude of L-type Ca^{2+} current (Ramos-Mondragon et al., 2012). However, until now, whether or how this drug can perturb different types of membrane ionic currents in electrically excitable cells is still poorly understood.

The magnitude of hyperpolarization-activated cation current (I_h or

* Corresponding author. Department of Physiology, National Cheng Kung University Medical College, No. 1, University Road, Tainan City, 70101, Taiwan.
E-mail addresses: cmcvecho2@gmail.com (W.-T. Chang), larry@mail.ncku.edu.tw (P.-Y. Liu), snwu@mail.ncku.edu.tw (S.-N. Wu).

https://doi.org/10.1016/j.ejphar.2020.173237
Received 8 April 2020; Received in revised form 26 May 2020; Accepted 29 May 2020
Available online 07 June 2020

funny current [I_f]) has been considered to be the notable determinant of repetitive electrical activities inherently in cardiac cells and various electrically excitable cells (DiFrancesco and DiFrancesco, 2015). This type of ionic current is characterized by a mixed inward Na^+/K^+ one with a slowly activating property during long-lasting membrane hyperpolarization, and it is subject either to inhibition by various compounds, such as CsCl, ivabradine, zatebradine or *ent*-kaurane-type diterpenoids, or to stimulation by oxaliplatin (DiFrancesco and DiFrancesco, 2015; Tanguay et al., 2019; Van Bogaert and Pittoors, 2003).

As described previously (Chang et al., 2019; Irisawa et al., 1993; Stojilkovic et al., 2017), the increased amplitude of I_h can depolarize membrane potential to the threshold required for action potential elicitation in electrically excitable cells. The I_h has been observed to be carried by channels of the hyperpolarization-activated cyclic nucleotide-gated (HCN1-4) gene family, a member of cyclic nucleotide-gated and voltage-gated K^+ channels (Ciotu et al., 2019; DiFrancesco and DiFrancesco, 2015). However, to the best of our knowledge, limited information regarding effects of PFD on the biophysical and pharmacological properties of I_h has been reported.

Therefore, in light of the considerations described above, the current study wanted to explore whether PFD is capable of interacting with HCNx channels to perturb any modifications on I_h in a concentration- and state-dependent fashion and to determine whether this compound exerts any perturbations on different types of K^+ currents (e.g., M-type K^+ current [$I_{K(M)}$] and *erg*-mediated K^+ current [$I_{K(erg)}$]) or L-type Ca^{2+} current ($I_{Ca,L}$) in pituitary tumor (GH_3) cells, a well-characterized and stable electrically excitable cell model.

2. Materials and Methods

2.1. Cell culture

Pituitary tumor (GH_3) cells, acquired from the Bioresources Collection and Research Center ([BCRC-60015], https://catalog.bcrc.firdi.org.tw/BcrcContent?bid=60015]; Hsinchu, Taiwan), were grown in Ham's F-12 medium supplemented with 2.5% (v/v) fetal calf serum, 15% (v/v) horse serum, and 2 mM L-glutamine, in a humidified atmosphere of 5% CO_2 and 95% air at 37 °C. Subcultures were obtained by trypsinization (0.025% trypsin solution [HyClone™] containing 0.01% sodium *N*,*N*-diethyldithiocarbamate and EDTA). The experiments were conducted five days after cells were culture up to 60–80% confluence. The chemical, drugs, and solutions used were listed in **Supplementary Materials and Methods.**

2.2. Electrophysiological measurements

Immediately before the measurements were performed, cells were harvested with 1% trypsin/EDTA solution and an aliquot of cell suspension was carefully transferred to a home-made recording chamber which was firmly placed on the stage of an inverted DM-IL microscope (Leica; Major Products, New Taipei City, Taiwan). During the experiments, cells were adhered to the chamber bottom at room temperature (20–25 °C) in HEPES-buffered normal Tyrode's solution. To prepare the patch electrodes from Kimax-51 capillary tubes (#34500; Kimble, Dogger, New Taipei City, Taiwan), either a PP-83 vertical puller (Narishige; Taiwan Instrument, Tainan, Taiwan) or a P-97 Flaming/Brown horizontal puller (Sutter: Taiwan Instrument, Tainan, Taiwan) was used; the tips were fire-polished with MF-83 microforge (Narishige). During the recordings, the electrodes, which bore resistances between 3 and 5 MΩ as filled with different internal solutions described above, were maneuvered by using an MX-4 manipulator (Narishige) and then finely operated by an MHW-3 hydraulic micromanipulator (Narishige). Standard patch-clamp recordings in the whole-cell configuration were undertaken by using either an RK-400 (Bio-Logic, Claix, France) or Axopatch-200B (Molecular Devices; Advance Biotech, New Taipei City, Taiwan) amplifier (Wu et al., 2017). Giga-seals were generally achieved in an all-or-nothing fashion and resulted in a dramatic improvement in signal-to-noise ratio. Liquid junction potentials, which developed at electrode tip as there is a difference of the composition between the internal and the bath solutions, were nulled shortly prior to the seal formation. According to such potentials, the whole-cell data was corrected.

The signals of voltage and current tracings were simultaneously monitored and digitally stored at 10 kHz in an ASUSPRO-BU401LG computer (ASUS, Tainan, Taiwan) and data acquisition was achieved by pCLAMP 10.7 software (Molecular Devices). To minimize electrical noise, the current signals collected were low-pass filtered at 3 kHz. Through digital-to-analog conversion, the pCLAMP-generated voltage profiles including various types of rectangular or triangular waveforms were specifically designed and then delivered to evaluate either the current-voltage (*I–V*) relationships of the current, or voltage hysteresis of ionic currents specified. The details of Data analyses were displayed in **Supplementary Materials and Methods.**

2.3. Statistical analyses

The nonlinear Hill or Boltzmann equation was fit to experimental results either by using the Excel Solver (Microsoft, Redmond, WA), OriginPro 2016 (OriginLab; Schmidt, Taipei, Taiwan), or MathCad Prime 5.0 (Linksoft, New Taipei City, Taiwan). The activation, inactivation or deactivation time course of the current specified was fit either to single- or double-exponential function. The voltage- or current-clamp data are expressed as the mean ± S.E.M with sample sizes (n) indicating the cell number from which the data were carefully collected, and error bars were plotted as S.E.M. In the present study, as the assertions were made with respect to the variability of mean, the Student's *t*-test (for paired or unpaired samples), or one-way analysis of variance (ANOVA) followed by *post-hoc* Fisher's least-significant difference test was implemented for the statistical evaluation of differences among means. When the normality underlying ANOVA was assumed to be violated, the non-parametric Kruskal-Wallis test was used. All statistical calculations were performed with SPSS 17.0 (AsiaAnalytics, Taipei, Taiwan). Values of $P < 0.05$ were statistically considered significant, unless otherwise stated.

3. Results

3.1. Effect of PFD on hyperpolarization-activated cation current (I_h) identified in pituitary GH_3 cells

In initial experiments, the modification of I_h caused by PFD in GH_3 cells was evaluated. Cells were bathed in Ca^{2+}-free Tyrode's solution, where Ca^{2+}-activated K^+ currents are mostly diminished, and the recording electrode was backfilled by using K^+-containing isotonic solution. With the established whole-cell current recordings (i.e., membrane patch under the electrode was broken by gentle suction), the examined cells were voltage-clamped at the level of −40 mV, and a long-lasting membrane hyperpolarization to −110 mV was delivered. Under this experimental protocol, a large and slowly developing inward current activated in response to 2-s-long hyperpolarizing step was readily evoked, and regarded as an I_h (Irisawa et al., 1993; Simasko and Sankaranarayanan, 1997). After 1 min of continuous exposure of cell to PFD, a concentration-dependent decrease in the amplitude of I_h was observed, in combination with a considerable slowing in activation and deactivation rate of the current (Fig. 1A). For example, the presence of 3 μM PFD produced a decline in current amplitude at the end of hyperpolarizing step from 73.5 ± 9.7 to 37.2 ± 4.2 pA (n = 9, $P < 0.05$). Post the compound was washed out, current amplitude returned to 70.5 ± 8.5 pA (n = 9). Besides, apart from the depressed I_h amplitude, the value of activation time constant (τ_{act}) of the current, in response to sustained hyperpolarization, was evidently raised during

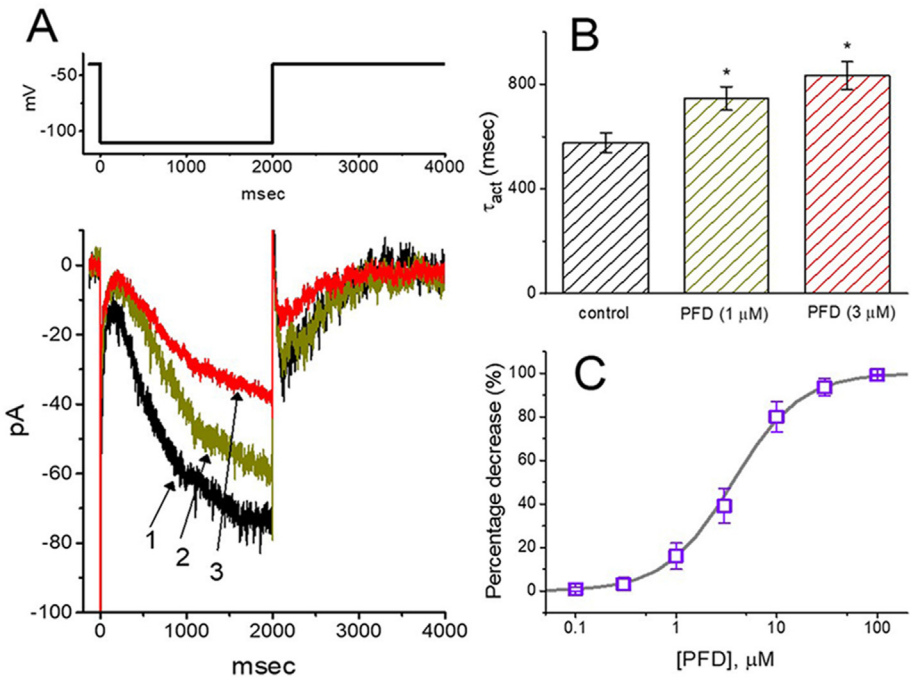

Fig. 1. Effect of PFD on hyperpolarization-activated cation current (I_h) measured from pituitary GH_3 cells. **(A)** Representative I_h traces obtained in the absence (1) and presence of 1 μM PFD (2) or 3 μM PFD (3). The upper part shows the voltage protocol applied. **(B)** Summary bar graph showing the effect of PFD (1 and 3 μM) on the activation time constant (τ_{act}) of I_h in response to step hyperpolarization applied from −40 to −110 mV with a duration of 2 s (mean ± S.E.M; n = 9 for each bar). *, Significantly different from control ($P < 0.05$). **(C)** Concentration-dependent inhibition of PFD on I_h in response to membrane hyperpolarization (mean ± S.E.M; n = 8 for each point). Current amplitude was taken at the end of 2-s hyperpolarizing pulse applied from −40 to −110 mV. The modified Hill equation detailed under **Materials and Methods** was reasonably fit to the experimental data (solid line).

exposure to the compound (Fig. 1A and B). For example, the application of 3 μM PFD to the bath was effective at increasing the τ_{act} value to 834 ± 54 ms (n = 9, $P < 0.05$) from a control value of 576 ± 38 ms (n = 9).

The depressant effect of PFD with different concentration on I_h elicited by 2-s-long sustained hyperpolarization was further examined. The concentration-dependent relationship of the inhibitory effect of this compound on I_h amplitude in GH_3 cells is illustrated in Fig. 1C. According to the Hill equation indicated under **Materials and Method**, the IC_{50} value of PFD which was needed for the inhibition of I_h was thereafter calculated to be 3.65 μM with the Hill coefficient of 1.3.

3.2. Comparisons among the depressant effects of ivabradine, ivabradine plus PFD, zatebradine, zatebradine plus PFD on I_h amplitude

Next, whether the subsequent addition of PFD, but still in the continued presence of ivabradine or zatebradine, was able to perturb the block by ivabradine or zatebradine of I_h inherently in GH_3 cells was investigated. Ivabradine or zatebradine has been reported to decrease HCN-encoded currents effectively (Chang et al., 2019; DiFrancesco and DiFrancesco, 2015; Novella Romanelli et al., 2016). As shown in Fig. 2, subsequent application of PFD (3 μM), still in the presence of either ivabradine (1 μM) or zatebradine (1 μM), was capable of producing an additional decline in I_h amplitude elicited by 2-s-long hyperpolarizing step. The experimental results obtained demonstrated that either ivabradine or zatebradine could act in concert with PFD to decrease I_h amplitude, and could thus be interpreted to indicate that both inhibitory effects of ivabradine or zatebradine and that of PFD on I_h amplitude appear to be additive in these cells.

3.3. Effect of PFD on the I–V relationship of I_h in GH_3 cells

The effect of PFD on I_h at various levels of membrane potentials was next investigated. The I_h was robustly evoked as the cell was hyperpolarized from −40 mV to a series of voltage steps ranging between −120 and −80 mV (Fig. 3A and B). The mean *I–V* relationships of I_h with or without PFD were established and hence depicted in Fig. 3B. With whole-cell conductance of I_h measured at the potentials ranging between −120 and −100 mV, the addition of 3 μM PFD was able to

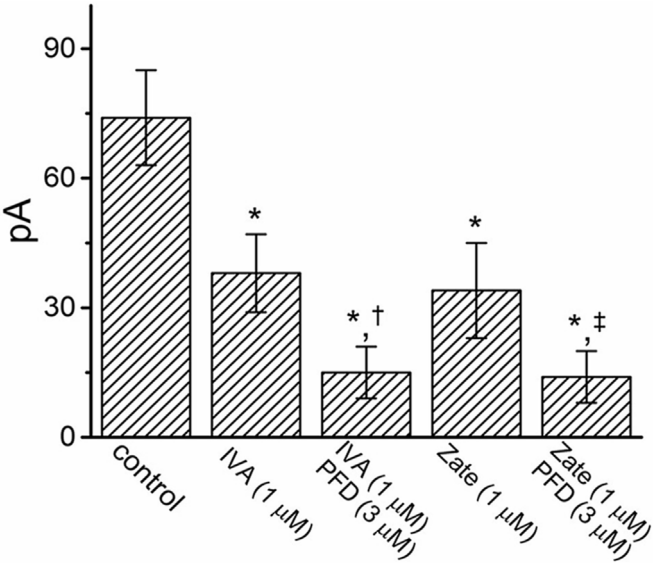

Fig. 2. Comparisons among depressant effects of ivabradine (IVA), zatebradine (Zate), ivabradine plus PFD, and zatebradine plus PFD on I_h amplitude in GH_3 cells (mean ± S.E.M; n = 8–9 for each bar). Current amplitudes were measured at the end of 2-s hyperpolarizing pulse applied from −40 mV abruptly to −110 mV. *, Significantly different from control ($P < 0.05$), †, significantly different from ivabradine (1 μM) alone group ($P < 0.05$), and ‡, significantly different from zatebradine (1 μM) alone group ($P < 0.05$).

diminish the I_h conductance from 4.62 ± 1.17 to 2.68 ± 0.09 nS (n = 8, $P < 0.05$).

3.4. Perturbation of the steady-state activation curve of I_h caused by PFD

To further investigate the inhibitory effect of PFD on I_h in GH_3 cells, the possible changes induced by this compound on the steady-state activation curve of I_h were studied. In these voltage-clamp experiments, a two-step voltage pulse was applied in situations where a 2-s conditioning pulse to various membrane potentials were delivered to precede the test pulse (2 s in duration) to −120 mV from −40 mV holding

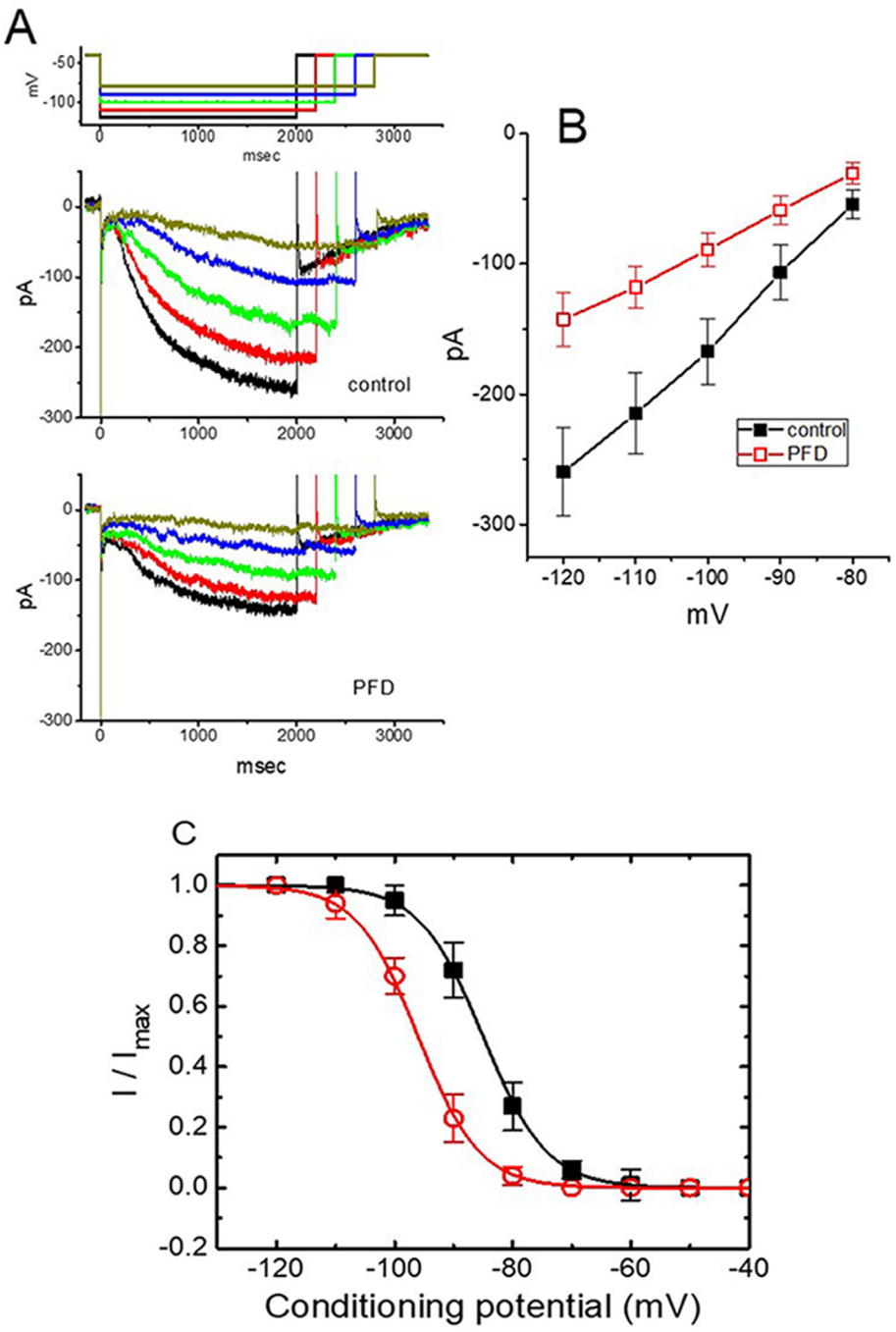

Fig. 3. Effect of PFD on mean current-voltage (*I–V*) relationships and the steady-state activation curve of I_h identified in GH_3 cells. **(A)** The uppermost graph depicts the voltage profile applied, the potential traces labeled in different colors correspond with current traces obtained with or without PFD addition; the duration in each hyperpolarizing step is different for better illustrations. Below are representative I_h traces obtained in the absence (upper) and presence of 3 μM PFD (lower). **(B)** Mean *I–V* relationships of I_h amplitude in the absence (■) and presence (□) of 3 μM PFD (mean ± S.E.M; n = 8 for each point). Current amplitude was taken at the end of each hyperpolarizing step. **(C)** The steady-state activation curve of I_h obtained in the control (■) and during exposure to 3 μM PFD (○) detected in GH_3 cells (mean ± S.E.M; n = 8 for each point). The continuous smooth lines overlaid on the data points show the least-squares fit to the Boltzmann equation indicated in **Materials and Methods**.

potential. Fig. 3C illustrates the relationship between the conditioning potentials versus the normalized amplitudes (I/I_{max}) of I_h obtained with or without PFD (3 μM). The data satisfactorily fitted to a Boltzmann function, as defined in **Materials and Methods**. In control, $V_{1/2} = -85 \pm 3$ mV, q = 4.7 ± 0.4 *e* (i.e., elementary charges) (n = 8), whereas in the presence of 3 μM PFD, $V_{1/2} = -96 \pm 4$ mV, q = 4.8 ± 0.4 *e* (n = 8). The data suggest that the exposure to PFD not only decreases the maximal conductance of I_h, but overly shifts the activation curve along with the voltage axis to the negative potential by roughly 11 mV; however, there was devoid of changes in the gating charge of the curve in its presence.

3.5. Effect of PFD on the voltage hysteresis elicited responding to triangular ramp pulse

The voltage hysteresis of I_h has been shown with an impact on electrical behaviors of AP firing (Chang et al., 2020; Männikkö et al., 2005). Therefore, it was explored whether a possible voltage hysteresis exists in I_h measured from GH_3 cells and how the presence of PFD modifies such hysteresis. In this experiment, a long-lasting inverted triangular ramp pulse with a duration of 2 s (i.e., ± 0.1 V/s) was delivered in the whole-cell configuration. Of interest, as can be seen in Fig. 4A, the trajectories of I_h elicited by the downsloping (i.e., hyperpolarized from −50 to −150 mV) and upsloping (i.e., depolarizing from −150 to −50 mV) ramp pulse as a function of time were overly distinguishable between these two limbs. The downsloping (forward) limb elicited current amplitude of the inverted triangular voltage ramp

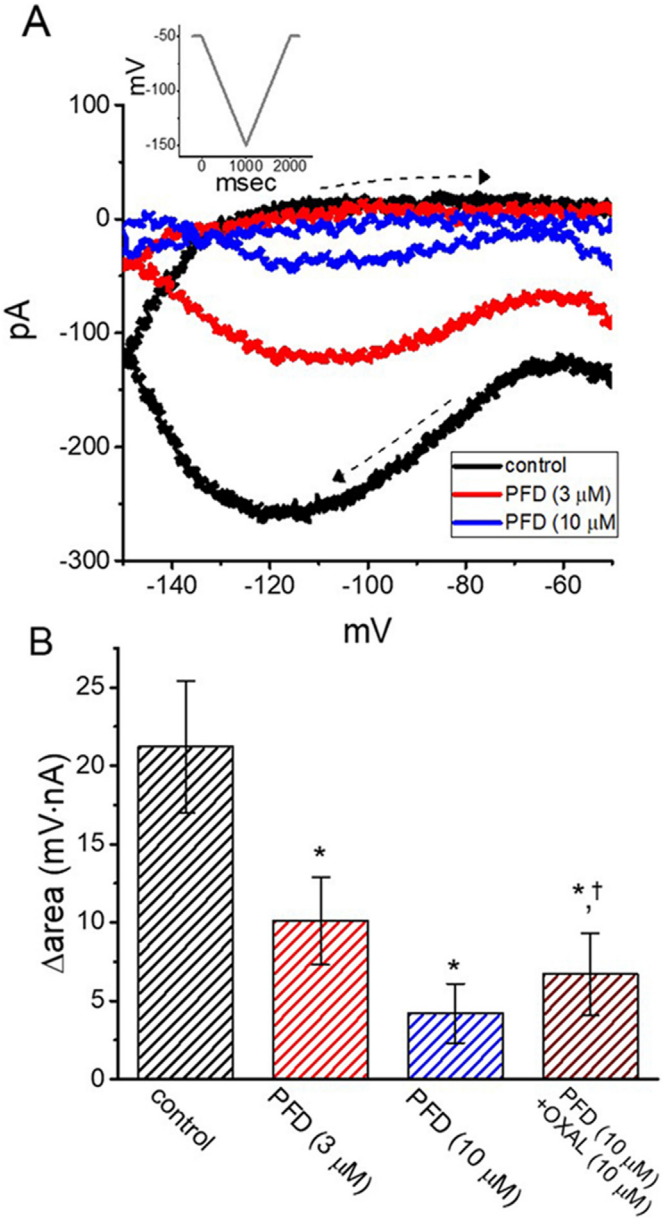

Fig. 4. Effect of PFD on the voltage hysteresis of I_h identified from GH_3 cells. **(A)** Representative I_h traces in the absence and presence of 3 or 10 μM PFD. Current traces were elicited in response to 2-s long inverted triangular (i.e., downsloping and upsloping) ramp pulse applied between −50 and −150 mV. Inset denotes the inverted triangular ramp pulse given, and the dashed arrows denote the direction of I_h in which time passes. **(B)** Summary bar graph showing the effect of PFD (3 or 10 μM) and 10 μM PFD plus oxaliplatin (OXAL, 10 μM) on the Δarea of voltage hysteresis (mean ± S.E.M; n = 8 for each bar). *, Significantly different from control ($P < 0.05$) and †, significantly different from PFD (10 μM) alone group ($P < 0.05$).

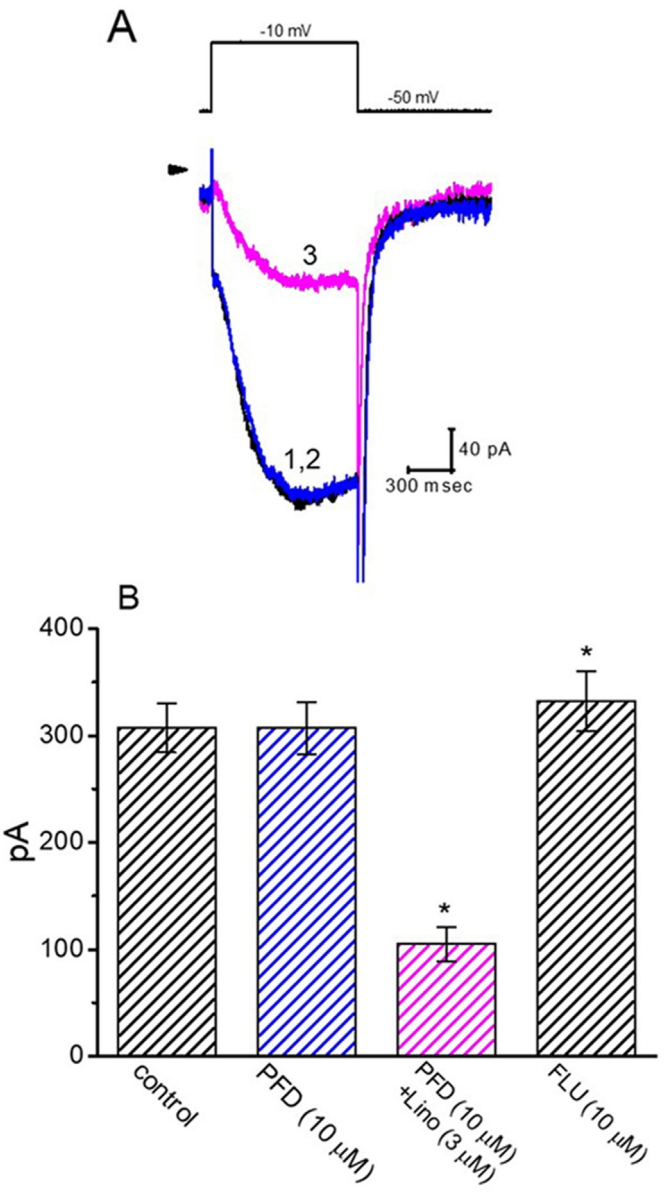

Fig. 5. Failure of PFD to modify M-type K^+ current ($I_{K(M)}$) identified in GH_3 cells. In the current voltage-clamp experiments, cells were bathed in high-K^+, Ca^{2+}-free solution and the recording electrode was filled with K^+-containing solution. **(A)** Representative $I_{K(M)}$ traces in response to step depolarization (indicated in the upper part) were obtained in control (1), after cell exposure to 10 μM PFD (2), and after addition of 10 μM PFD plus 10 μM linopirdine (3). Arrowhead is the zero-current level and calibration mark shown at the right lower corner applied to all current traces. **(B)** Summary bar graph showing effect of PFD, PFD plus linopirdine, and flupirtine on $I_{K(M)}$ amplitude in these cells (mean ± S.E.M; n = 9 for each bar). The $I_{K(M)}$ amplitude was measured at the end of the depolarizing step from −50 to −10 mV. *, Significantly different from control ($P < 0.05$).

was lower than that by the upsloping (backward) limb, strongly indicating that there was a voltage hysteresis for this current in these cells. As the ramp speed was reduced, the hysteretic magnitude for I_h became progressively increased. The degree of voltage hysteresis was quantified according to the difference in area under the curve in the forward (downsloping) and reverse (upsloping) direction, as denoted by the arrows in Fig. 4A. The data indicate that for I_h in GH_3 cells, the degree of voltage hysteresis increases with slower ramp speed, and that cell exposure to PFD leads to a substantial reduction in the amount of such hysteresis.

In the experiments on PFD or PFD plus oxaliplatin on voltage hysteresis of I_h, a long-lasting inverted triangular ramp pulse with a duration of 2 s (i.e., ± 0.1 V/s) was undertaken in the whole-cell configuration. Fig. 4B illustrates a summary of the data showing the effects of PFD and PFD plus oxaliplatin on the area (i.e., Δarea) under the curve between the forward and backward current traces. For example, the addition of PFD (3 μM) reduced the area up to 55%, elicited by the long-lasting inverted triangular voltage ramp. The PFD-mediated reduction in the magnitude of voltage hysteresis of I_h could be significantly reversed by adding oxaliplatin (10 μM). Oxaliplatin, a chemotherapeutic antineoplastic agent, has been previously reported to

activate I_h (Chang et al., 2020).

3.6. Failure of PFD to affect M-type K^+ current ($I_{K(M)}$) in GH_3 cells

It was additionally evaluated whether the presence of PFD produces any effects on different types of K^+ currents (e.g., $I_{K(M)}$) present in these cells. To measure $I_{K(M)}$, GH_3 cells were bathed in high-K^+, Ca^{2+}-free solution with the recording pipette filled with K^+-containing solution. The examined cell was voltage-clamped at −50 mV and sustained depolarization to −10 mV was applied (Selyanko et al., 1999; So et al., 2019). As illustrated in Fig. 5A and B, PFD at a concentration of 10 μM did not alone produce any effect on $I_{K(M)}$ responding to maintained depolarization applied from −50 to −10 mV. However, as 10 μM PFD was continually present, subsequent application of linopirdine (3 μM) noticeably decreased I_h amplitude effectively, notwithstanding the ability of flupirtine (10 μM) alone to enhance current amplitude (Fig. 5B). Linopirdine can inhibit $I_{K(M)}$, while flupirtine has been reported to enhance $I_{K(M)}$ (Hsu et al., 2014; Pattnaik and Hughes, 2012).

3.7. Inability of PFD to modify erg-mediated K^+ current ($I_{K(erg)}$) in GH_3 cells

In another set of experiments, whether another type of K^+ current, namely $I_{K(erg)}$, would be subject to perturbations by PFD was also further examined. With cells bathed in high-K^+, Ca^{2+}-free solution and the pipette were filled with K^+-containing solution (Huang et al., 2011; So et al., 2019). As shown in Fig. 6A and B, cell exposure to 10 μM PFD did not perturb the amplitude of deactivating $I_{K(erg)}$ elicited by membrane hyperpolarization as reported previously (So et al., 2019). For example, as the cells were 1-s hyperpolarized to −90 mV from a holding potential of −10 mV, the peak amplitude of $I_{K(erg)}$ did not differ significantly between the absence and presence of 10 μM PFD (742 ± 43 pA [control] versus 739 ± 45 pA [in the presence of 10 μM PFD]; n = 9, $P > 0.05$). Moreover, further application of BeKM-1 (1 μM), but still in the continued presence of PFD, was effective at decreasing $I_{K(erg)}$, as demonstrated by the significant reduction of $I_{K(erg)}$ amplitude to 328 ± 23 pA (n = 9, $P < 0.05$). BeKm-1 is a scorpion toxin reported to suppress $I_{K(erg)}$ effectively in heart cells and to prolong QT interval in isolated rabbit heart (Korolkova et al., 2001; Qu et al., 2011). It is conceivable, therefore, that $I_{K(M)}$ or $I_{K(erg)}$ observed in GH_3 cells is resistant to any modifications by PFD.

3.8. Depressive effect of PFD on L-type Ca^{2+} current ($I_{Ca,L}$) in GH_3 cells

Early studies have demonstrated the ability of PFD to augment the amplitude of $I_{Ca,L}$ in heart cells (Ramos-Mondragon et al., 2012). Therefore, it was further evaluated if PFD could modify the amplitude or gating of $I_{Ca,L}$ present in this lactotroph cell model. Previous reports have demonstrated the presence of L-type Ca^{2+} currents functionally expressed in pituitary GH_3 cells (Huang et al., 2019; Lo et al., 2001). To achieve these objectives, in a separate set of whole-cell voltage-clamp experiments, cells were bathed in normal Tyrode's solution, which consists of 1.8 mM $CaCl_2$, 10 mM tetraethylammonium chloride, and 1 μM tetrodotoxin, and the recording pipette was filled with a Cs^+-containing solution. As can be seen in Fig. 7A, PFD (3 or 10 μM) decreased the peak amplitude of $I_{Ca,L}$ elicited by the 300-ms depolarizing pulse from −40 to 0 mV. However, no obvious changes were observed in the activation or inactivation time course of $I_{Ca,L}$ elicited responding to the abrupt step depolarization. Furthermore, as the clamp pulses of 300-ms duration from −40 mV to various membrane potentials were applied, the overall *I–V* relationship of peak $I_{Ca,L}$ seen with these cells virtually was not perturbed by the presence of PFD (10 μM) (Fig. 7B). As such, distinct from previous reports in heart cells (Ramos-Mondragon et al., 2012), the present results demonstrate that PFD exerts a depressant action of the peak $I_{Ca,L}$ in GH_3 cells.

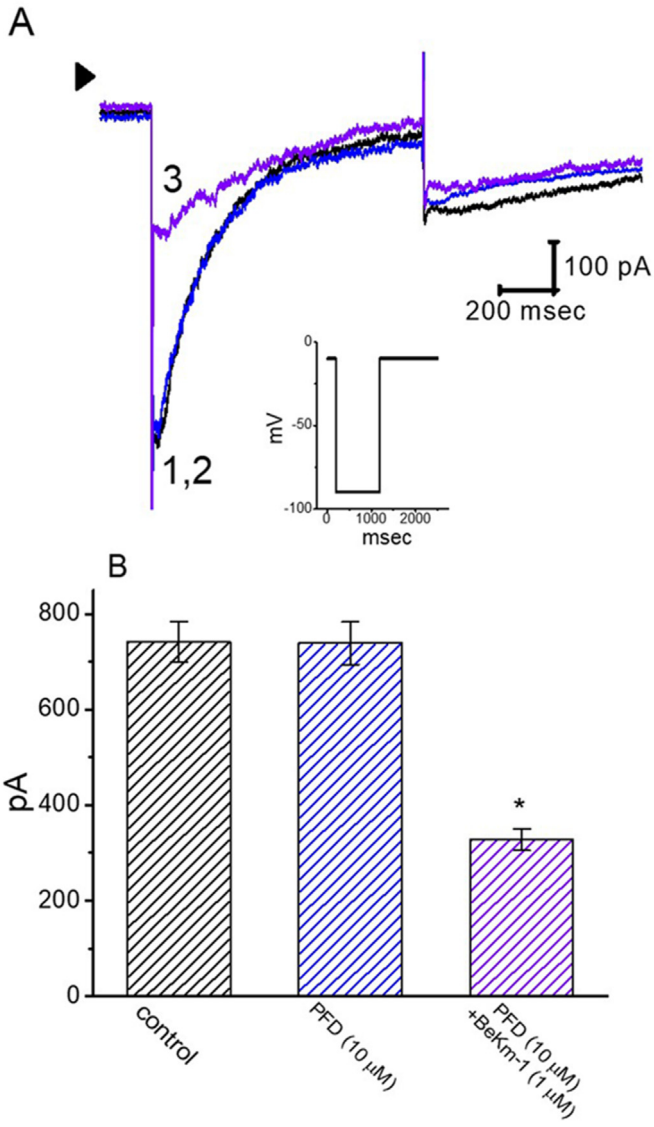

Fig. 6. Inability of PFD to alter the amplitude of *erg*-mediated K^+ current ($I_{K(erg)}$) in GH_3 cells. The experiments were performed in situations where cells were bathed in high-K^+, Ca^{2+}-free solution and the pipette was backfilled with K^+-containing solution. **(A)** Representative $I_{K(erg)}$ traces obtained in the control (i.e., PFD was not present) (1), after addition of 10 μM PFD (2), or 10 μM PFD plus 1 μM BeKm-1 (3). Inset indicates the voltage protocol given, arrowhead is the zero-current level and calibration mark applies to all current traces. **(B)** Summary bar graph showing the effect of PFD and PFD plus BeKm-1 on the amplitude of deactivating $I_{K(erg)}$ in these cells (mean ± S.E.M; n = 8 for each bar). The $I_{K(erg)}$ amplitude was measured at the beginning of 1-s-long hyperpolarizing step applied from −10 to −90 mV. *, Significantly different from control or PFD (10 μM) alone group ($P < 0.05$).

3.9. Effect of PFD on the firing of spontaneous action potentials (APs) in GH_3 cells

In a separate set of experiments, the model was switched to whole-cell current-clamp conditions where, as the cell was clamped at 0 current, any changes in membrane potential can be thereafter measured. During such potential recordings, cells were immersed in normal Tyrode's solution which consists of 1.8 mM $CaCl_2$ and the pipette was filled with K^+-containing internal solution. As depicted in Fig. 8A and B, cell exposure to PFD resulted in a progressive decline in the firing frequency of regenerative APs. For instance, the exposure to PFD at a concentration of 1 or 3 μM greatly decreased discharge rate of current-

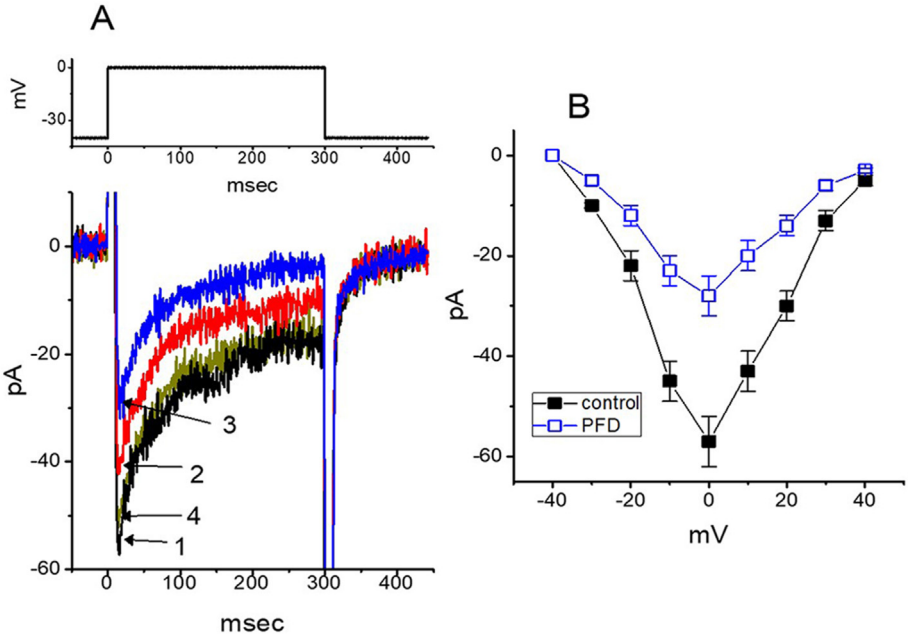

Fig. 7. Effect of PFD on L-type Ca^{2+} current ($I_{Ca,L}$) in GH_3 cells. The experiments were conducted in cells bathed in normal Tyrode's solution which contained 1.8 mM $CaCl_2$, and the recording pipette was backfilled with Cs^+-containing solution. **(A)** Representative $I_{Ca,L}$ traces taken in the control (1), during the exposure to 3 μM PFD (2) or 10 μM PFD (3), and after washout of PFD (4). The inwardly directed $I_{Ca,L}$ was evoked by the depolarizing pulse as indicated in the upper part. **(B)** Mean *I–V* relationships of peak $I_{Ca,L}$ in the absence (■) and presence (□) of 10 μM PFD (mean ± S.E.M; n = 8 for each point). The current amplitude was measured at the beginning of each depolarizing pulse applied at various voltages. Note that the overall *I–V* relationship of peak I_{Ca} was not modified in the presence of PFD (10 μM).

clamped cells to 1.07 ± 0.07 Hz (n = 9, $P < 0.05$) or 0.74 ± 0.05 Hz (n = 9, $P < 0.05$), respectively, from a control value of 1.45 ± 0.09 Hz (n = 9). Meanwhile, the presence of zatebradine (3 μM) alone was noted to decrease firing frequency effectively. Zatebradine has previously been reported to be an inhibitor of I_h (Novella Romanelli et al., 2016; Romanelli et al., 2005; Van Bogaert and Pittoors, 2003). Therefore, it is conceivable from the current data that PFD-mediated modification in membrane potential tends to be intimately connected to its perturbations on both I_h and $I_{Ca,L}$ detected above in these cells.

3.10. Effect of PFD on sag voltage identified in GH_3 cells

In another stage of current-clamp recordings, the ability of PFD to induce perturbations on sag voltage was further investigated. The magnitude of such voltage responding to hyperpolarizing current injection has been reported linking to the emergence of I_h (Chang et al., 2019; Datunashvili et al., 2018). As depicted in Fig. 9A and B, under the current experimental conditions, when the whole-cell potential recordings were set up, the hyperpolarizing current injection at the amplitude of 25 pA was able to induce sag voltage (i.e., drop down to a lower level in the membrane potential applied by such hyperpolarizing current injection). The addition of chlorotoxin (1 μM), a blocker of Cl^- channels, was not found to exert any effect on the amplitude of sag voltage in response to hyperpolarizing current injection. On the other hand, as cells were exposed to PFD, the amplitude of sag voltage was decreased. For example, the addition of 1 μM PFD caused a reduction in the sag-voltage amplitude from 55 ± 13 to 36 ± 11 mV (n = 8, $P < 0.05$). Therefore, the depression of sag voltage caused by PFD can be ascribed in large part to its inhibitory effect on the amplitude and gating of I_h detected above in these cells.

4. Discussion

The I_h of pituitary GH_3 cells demonstrated in the present investigation can be observed following the 2-s-long hyperpolarizing pulse applied from −40 mV to the voltages more negative to −80 mV, and the currents were increased in both current amplitude and activation in response to more hyperpolarizing potentials (Chang et al., 2019; DiFrancesco and DiFrancesco, 2015; Irisawa et al., 1993; Simasko and Sankaranarayanan, 1997). The forward and backward amplitudes of this current elicited by long-lasting inverted triangular ramp pulse were also noted to be distinct, strongly reflecting the presence of voltage-dependent hysteresis fo I_h (Barthel et al., 2016; Männikkö et al., 2005). This major ion conductance inherently present in GH_3 lactotrophs was identified as an I_h or I_f current (Chang et al., 2019; Simasko and Sankaranarayanan, 1997). Specifically, this study shows for the first time the effectiveness of PFD in depressing the amplitude of I_h in a concentration - and voltage-dependent fashion.

In this study, the block by PFD on I_h in GH_3 cells are not strictly limited to its inhibition of the current amplitude. Concomitantly, as cells were exposed to PFD, the time course of I_h activation and deactivation, in response to sustained membrane hyperpolarization, apparently became slower. The presence of this compound was found to produce a decrease in I_h activation in a concentration- and time-dependent manner. The results thus prompted us to reflect that blocking of I_h by PFD inherently is not instantaneous, but develops with time after the HCN channel opened and subsequently produces a slowing in current activation. In other words, the PFD molecule tends to represent a higher affinity for the open state in the HCN channel; consequently, the transition from closed to open state turns out to be slower during cell exposure to PFD. It is thus possible that PFD or its structurally related compounds bind to the open state of the channel and/or block a prolonged channel opening.

The steady-state activation curve of I_h detected in this study was shifted along the voltage axis toward a negative voltage in the presence of PFD. However, failure of PFD to change the gating charge of the current in situations where the transmembrane electrical field can be crossed during current activation, suggests that PFD action on the HCN channel might consist in opening the gate, not interfering with the region that senses the transmembrane potential. Nonetheless, the sensitivity of electrically excitable cells to PFD could rely not simply on the PFD concentrations given, but also the pre-existing level of the resting potential, the firing pattern of APs, or their combinations, assuming the magnitude of I_h is present in the cells examined.

Voltage-dependent hysteresis of I_h is considered to serve a role in influencing the overall behaviors of electrically excitable cells including GH_3 cells. In accordance with previous observations ((Barthel et al., 2016; Chang et al., 2020; Männikkö et al., 2005), the I_h natively in GH_3 cells has been described either to undergo a hysteretic perturbation in its voltage dependence, or to produce a shift of ion-channel mode in which the voltage sensitivity in gating charge movement of the current

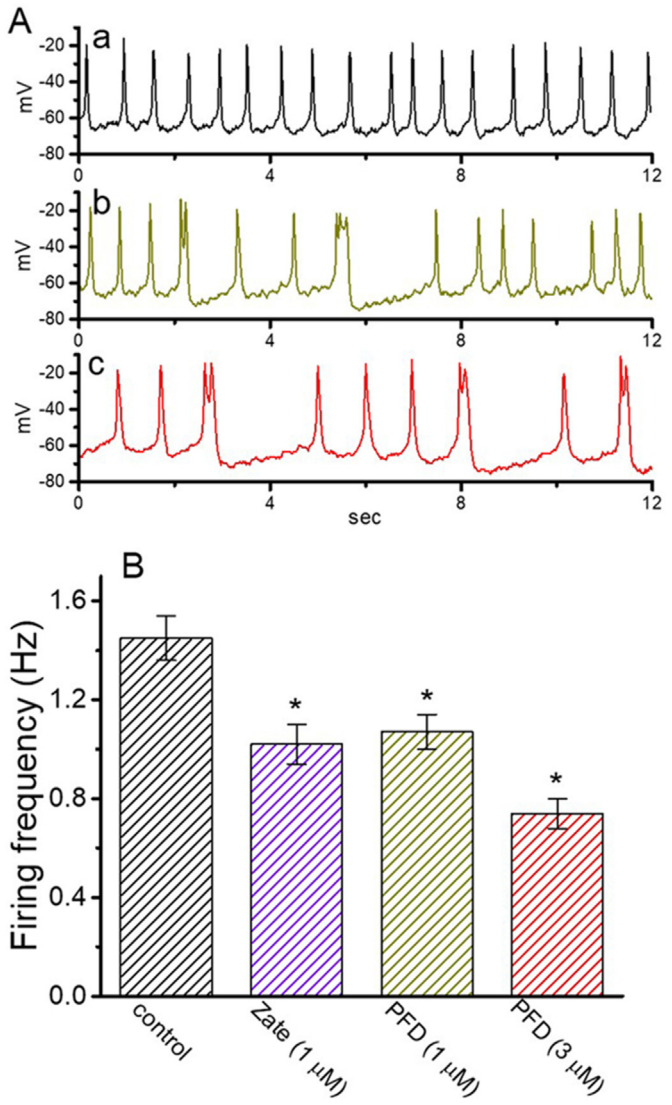

Fig. 8. Effect of PFD on regenerative actions potentials (APs) identified in GH_3 cells. The set of current-clamp potential recordings in this and the following Figure was conducted in situations where cells were bathed in normal Tyrode's solution containing 1.8 mM $CaCl_2$ and the recording electrode was filled with K^+-containing solution. As whole-cell configuration was established, the recoding mode was rapidly switched to current-clamp conditions for measuring changes in membrane potential. **(A)** Representative potential traces obtained in the control (a) and during cell exposure to 1 μM PFD (b) or 3 μM PFD (c). **(B)** Summary bar graph showing the inhibitory effectiveness of PFD or zatebradine (Zate) on the firing frequency of regenerative APs in GH_3 cells (mean ± S.E.M; n = 9 for each bar). *, Significantly different from control ($P < 0.05$).

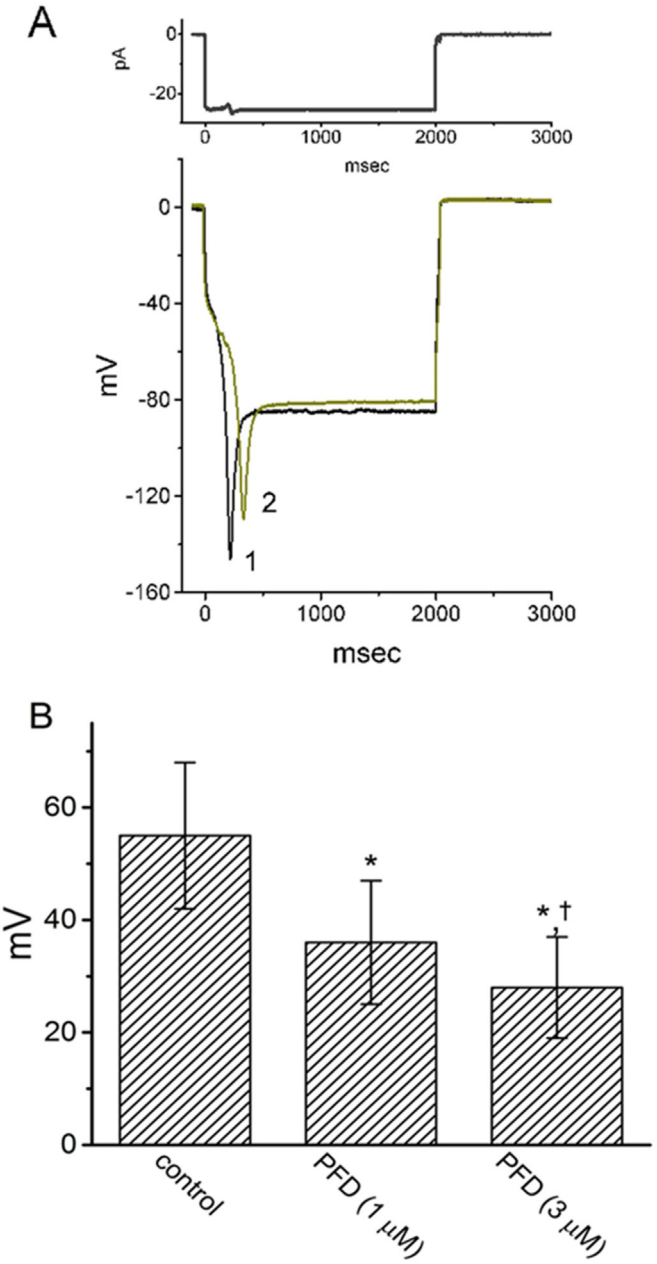

Fig. 9. Effect of PFD on sag voltage identified in GH_3 cells. As the whole-cell recordings were achieved, the experiment was rapidly switched to current-clamp configuration with 2-s hyperpolarizing current stimuli. **(A)** Potential traces obtained in the absence (1) and presence (2) of 1 mM PFD. The upper part is the current stimulus applied. **(B)** Summary bar graph showing inhibitory effect of PFD on the amplitude of sag voltage in these cells (mean ± S.E.M; n = 8). *, Significantly different from control ($P < 0.05$) and †, significantly from 1 μM PFD alone group ($P < 0.05$).

is dependent on the previous state of the HCN channel involved (Fürst and D'Avanzo, 2015; Männikkö et al., 2005). In the present study, we also investigated the perturbations of PFD on non-equilibrium property of I_h consistently observed in GH_3 cells. In this regard, because of a reduction in Δarea of hysteretic loop between forward and backward limp of the inverted triangular ramp pulse, the experimental data suggest that the presence of this compound is capable of diminishing such hysteresis entailed in the voltage-dependent elicitation of I_h.

The PFD concentration required for the half-maximal inhibition of I_h detected in this study was optimally determined to be 3.65 μM, a value which was within the clinically applied doses reported previously. For example, following intravenous administration of PFD, plasma concentration of this compound was previously reported to range between 0.1 and 10 μg/ml (i.e., 0.54 and 54 μM) (Togami et al., 2015). Alternatively, recent investigations reported the utilization of drug-delivery vehicles (e.g., nanoparticles) to facilitate specific delivery of PFD to the target organs (Ji et al., 2017; Maslanka Figueroa et al., 2020). In this scenario, the observed effects by PFD presented herein may achieve the concentration of clinical requirements, so that maneuvers are implemented to mitigate the systemic toxicity.

Ivabradine or zatebradine, known to inhibit HCN-encoded currents, have been previously reported to reduce diastolic dysfunction and later to ameliorate cardiac fibrosis in animal models (Busseuil et al., 2010; Fang et al., 2017). In our study, subsequent addition of PFD, still in the continued presence of this compound, can further depress I_h amplitude.

As such, the inhibitory effect of ivabradine (or zabebradine) and PFD on I_h detected in GH_3 cells could be additive. The elucidation whether the specific pharmacological interaction between the compounds is additive or even synergistic would require a more specific approach (i.e. isobolographic assessment), which is beyond the scope of the present study. Alternatively, further application of TGF-β (1 μM) had no modifications on PFD-mediated depression of I_h (data not shown). A previous study revealed the I_h functionally expressed in vascular smooth myocytes (Greenwood et al., 2001). A caveolin-binding domain existing in the HCN4 channels has been also reported to mediate the functional interaction with caveolin proteins (Barbuti et al., 2012). Therefore, to what extent PFD-mediated depression of I_h participates in its antifibrotic activity remained to be further resolved. Whether PFD-mediated block of I_h potentially contributes to its cardioprotective action described previously (Aimo et al., 2020; Fang et al., 2017; Nguyen et al., 2010) also needs further detailed investigations.

It is important to mention, from the present observations, that unlike its depressant effectiveness on $I_{Ca,L}$, block of I_h caused by PFD tends to be not instantaneous, but develops with time after the HCN channels become overly opened upon sustained membrane hyperpolarization, thereby producing a conceivable increase in τ_{act} value detected from whole-cell current activation. In the presence of this compound, deactivating current of I_h was also notably observed to exhibit a blunted peak followed by a slowing in the decay, reflecting that the closing (i.e., deactivating process) of channels virtually became slower by unbinding of the PFD molecule. PFD or its structurally similar compounds may hence be an intriguing tool to probe HCNx channels in the structural and functional perspectives, given that the pore region of the channel protein to which they bind appears to be of particular relevance for an open-channel blockade.

The present observations revealed the effectiveness of PFD on the decline in the firing frequency of spontaneous APs observed under current-clamp potential measurements. The amplitude of sag voltage elicited by 2-s hyperpolarizing current stimuli was also decreased in its presence. The inhibition by PFD of I_h amplitude and gating may confer its effectiveness on different cellular functions (e.g., stimulus-secretion coupling) in various types of electrically excitable cells (Lee et al., 2017; Stojilkovic et al., 2017; Zhang et al., 2008). Whether similar findings occur in different types of native cells *in vivo* still remains to be further delineated.

It is also important to emphasize that the treatment with PFD has been described to enhance the peak amplitude of $I_{Ca,L}$ in heart cells (Ramos-Mondragon et al., 2012). However, in the present study, vastly different from the depressant action of PFD on I_h, the addition of this compound was able to decrease the peak $I_{Ca,L}$ detected in GH_3 cells. Moreover, neither activation nor inactivation time course of the current by abrupt membrane depolarization presumably was not modified. A previous study has indeed reported that quercetin, a bioflavonoid, could either increase or decrease the amplitude of $I_{Ca,L}$ in different types of electrically excitable cells (Wu et al., 2003). Nonetheless, in combination with the depression of I_h, PFD-mediated depression of $I_{Ca,L}$ might also contribute to its effectiveness in altering functional activities of endocrine or neuroendocrine cells (Lee et al., 2017), despite inability of PFD to alter the amplitude of $I_{K(M)}$ or $I_{K(erg)}$. However, how PFD-perturbed changes on I_h or other ionic currents demonstrated here could be linked to its pathological or morphological changes (e.g., fibrosis) remained to be further studied.

5. Conclusions

Taken together, these results suggest that PDF is able to produce a decrease in I_h activation in a concentration-dependent manner. Also, the substance presents the characteristic of opening HCN channel and counteracting a prolonged channel opening. Our findings on GH_3 cells shed light on the evidence that PFD perturbs specific ionic currents which may be linked to additional effects, potentially useful for therapeutic application, when elicited on different excitable cells.

Data availability

The datasets used in the current study are available on reasonable request.

Funding

The work described in this manuscript is supported jointly by National Cheng Kung University (NCKUH-10709001), Ministry of Education (D108-F2507), and Ministry of Science and Technology (MOST-108-2314-B-006-094), Taiwan.

CRediT authorship contribution statement

Wei-Ting Chang: Conceptualization, Writing - review & editing. **Eugenio Ragazzi:** Writing - original draft. **Ping-Yen Liu:** Visualization, Investigation. **Sheng-Nan Wu:** Writing - review & editing, Conceptualization, Data curation, Methodology, Software, Writing - review & editing.

Declaration of competing interest

The authors declare no competing financial interests.

Acknowledgements

The authors thank Zi-Han Gao and Sih-Wei Lee for the assistances in cell preparation.

Appendix A. Supplementary data

Supplementary data to this article can be found online at https://doi.org/10.1016/j.ejphar.2020.173237.

References

ClinicalTrials.gov [Internet], 2020 Mar 12. Identifier NCT04282902, A Study to Evaluate the Efficacy and Safety of Pirfenidone with Novel Coronavirus Infection. Available from National Library of Medicine (US), Bethesda (MD) : https://clinicaltrials.gov/ct2/show/NCT04282902?term=NCT04282902&draw=2&rank=1.

Aimo, A., Cerbai, E., Bartolucci, G., Adamo, L., Barison, A., Lo Surdo, G., Biagini, S., Passino, C., Emdin, M., 2020. Pirfenidone is a cardioprotective drug: mechanisms of action and preclinical evidence. Pharmacol. Res. 155, 104694.

Antoniu, S.A., 2006. Pirfenidone for the treatment of idiopathic pulmonary fibrosis. Expet Opin. Invest. Drugs 15, 823–828.

Balestro, E., Cocconcelli, E., Giraudo, C., Polverosi, R., Biondini, D., Lacedonia, D., Bazzan, E., Mazzai, L., Rizzon, G., Lococo, S., Turato, G., Tinè, M., Cosio, M.G., Saetta, M., Spagnolo, P., 2019. High-resolution CT change over time in patients with idiopathic pulmonary fibrosis on antifibrotic treatment. J. Clin. Med. 8, 1469.

Barbuti, A., Scavone, A., Mazzocchi, N., Terragni, B., Baruscotti, M., Difrancesco, D., 2012. A caveolin-binding domain in the HCN4 channels mediates functional interaction with caveolin proteins. J. Mol. Cell. Cardiol. 53, 187–195.

Barthel, L., Reetz, O., Strauss, U., 2016. Use dependent attenuation of rat HCN1-mediated Ih in intact HEK293 cells. Cell. Physiol. Biochem. 38, 2079–2093.

Busseuil, D., Shi, Y., Mecteau, M., Brand, G., Gillis, M.A., Thorin, E., Asselin, C., Romeo, P., Leung, T.K., Latour, J.G., Des Rosiers, C., Bouly, M., Rhéaume, E., Tardif, J.C., 2010. Heart rate reduction by ivabradine reduces diastolic dysfunction and cardiac fibrosis. Cardiology 117, 234–242.

Castro-Torres, R.D., Chaparro-Huerta, V., Flores-Soto, M.E., Banuelos-Pineda, J., Camins, A., Orozco-Suarez, S.A., Armendariz-Borunda, J., Beas-Zarate, C., 2014. A single dose of pirfenidone attenuates neuronal loss and reduces lipid peroxidation after kainic acid-induced excitotoxicity in the pubescent rat hippocampus. J. Mol. Neurosci. 52, 193–201.

Chang, W.T., Gao, Z.H., Lo, Y.C., Wu, S.N., 2019. Evidence for effective inhibitory actions on hyperpolarization-activated cation current caused by *Ganoderma* triterpenoids, the main active constituents of *Ganoderma* spores. Molecules 24, 4256.

Chang, W.T., Gao, Z.H., Li, S.W., Liu, P.Y., Lo, Y.C., Wu, S.N., 2020. Characterization in dual activation by oxaliplatin, a platinum-based chemotherapeutic agent of hyperpolarization-activated cation and electroporation-induced currents. Int. J. Mol. Sci. 21, 396.

Ciotu, C.I., Tsantoulas, C., Meents, J., Lampert, A., McMahon, S.B., Ludwig, A., Fischer, M.J.M., 2019. Noncanonical ion channel behaviour in pain. Int. J. Mol. Sci. 20, 4572.

Collins, B.F., Raghu, G., 2019. Antifibrotic therapy for fibrotic lung disease beyond idiopathic pulmonary fibrosis. Eur. Respir. Rev. 28, 190022.
Datunashvili, M., Chaudhary, R., Zobeiri, M., Luttjohann, A., Mergia, E., Baumann, A., Balfanz, S., Budde, B., van Luijtelaar, G., Pape, H.C., Koesling D, Budde T., 2018. Modulation of hyperpolarization-activated inward current and thalamic activity modes by different cyclic nucleotides. Front. Cell. Neurosci. 12, 369.
DiFrancesco, J.C., DiFrancesco, D., 2015. Dysfunctional HCN ion channels in neurological diseases. Front. Cell. Neurosci. 6, 174.
Fang, L., Murphy, A.J., Dart, A.M., 2017. A clinical perspective of anti-fibrotic therapies for cardiovascular disease. Front. Pharmacol. 8, 186.
Fürst, O., D'Avanzo, N., 2015. Isoform dependent regulation of human HCN channels by cholesterol. Sci. Rep. 5, 14270.
Greenwood, I.A., Ledoux, J., Leblanc, N., 2001. Differential regulation of Ca^{2+}-activated Cl^- currents in rabbit arterial and portal vein smooth muscle cells by Ca^{2+}-calmodulin-dependent kinase. J. Physiol. 534, 395–408.
Hsu, H.T., Tseng, Y.T., Lo, Y.C., Wu, S.N., 2014. Ability of naringenin, a bioflavonoid, to activate M-type potassium current in motor neuron-like cells and to increase BK_{Ca}-channel activity in HEK293T cells transfected with-hSlo subunit. BMC Neurosci. 15, 135.
Huang, M.H., Shen, A.Y., Wang, T.S., Wu, H.M., Kang, Y.F., Chen, C.T., Hsu, T.I., Chen, B.S., Wu, S.N., 2011. Inhibitory action of methadone and its metabolites on *erg*-mediated K^+ current in GH_3 pituitary tumor cells. Toxicology 280, 1–9.
Huang, M.H., Liu, P.Y., Wu, S.N., 2019. Characterization of perturbing actions by verteporfin, a benzoporphyrin photosensitizer, on membrane ionic currents. Front. Chem. 7, 566.
Irisawa, H., Brown, H.F., Giles, W., 1993. Cardiac pacemaking in the sinoatrial node. Physiol. Rev. 73, 197–227.
Ji, T., Lang, J., Wang, J., Cai, R., Zhang, Y., Qi, F., Zhang, L., Zhao, X., Wu, W., Hao, J., Qin, Z., Zhao, Y., Nie, G., 2017. Designing liposomes to suppress extracellular matrix expression to enhance drug penetration and pancreatic tumor therapy. ACS Nano 11, 8668–8678.
Kanayama, M., Mori, M., Matsumiya, H., Taira, A., Shinohara, S., Kuwata, T., Imanishi, N., Yoneda, K., Kuroda, K., Tanaka, F., 2020. Perioperative pirfenidone treatment for lung cancer patients with idiopathic pulmonary fibrosis. Surg. Today 50, 469–474.
Korolkova, Y.V., Kozlov, S.A., Lipkin, A.V., Pluzhnikov, K.A., Hadley, J.K., Filippov, A.K., Brown, D.A., Angelo, K., Strobaek, D., Jespersen, T., Olesen, S.P., Jensen, B.S., Grishin, E.V., 2001. An ERG channel inhibitor from the scorpion Buthus eupeus. J. Biol. Chem. 276, 9868–9876.
Krämer, M., Markart, P., Drakopanagiotakis, F., Mamazhakypov, A., Schaefer, L., Didiasova, M., Wygrecka, M., 2020. Pirfenidone inhibits motility of NSCLC cells by interfering with the urokinase system. Cell. Signal. 65, 109432.
Lee, E., Ryu, G.R., Ko, S.H., Ahn, Y.B., Song, K.H., 2017. A role of pancreatic stellate cells in islet fibrosis and beta-cell dysfunction in type 2 diabetes mellitus. Biochem. Biophys. Res. Commun. 485, 328–334.
Lo, Y.K., Wu, S.N., Lee, C.T., Li, H.F., Chiang, H.T., 2001. Characterization of action potential waveform-evoked L-type calcium currents in pituitary GH3 cells. Pflügers Archiv 442, 547–557.
Männikkö, R., Pandey, S., Larsson, H.P., Elinder, F., 2005. Hysteresis in the voltage dependence of HCN channels: conversion between two modes affects pacemaker properties. J. Gen. Physiol. 125, 305–326.
Maslanka Figueroa, S., Fleischmann, D., Beck, S., Goepferich, A., 2020. Thermodynamic, spatial and methodological considerations for the manufacturing of therapeutic polymer nanoparticles. Pharm. Res. (N. Y.) 37, 59.
Nguyen, D.T., Ding, C., Wilson, E., Marcus, G.M., Olgin, J.E., 2010. Pirfenidone mitigates left ventricular fibrosis and dysfunction after myocardial infarction and reduces arrhythmias. Heart Rhythm 7, 1438–1445.
Novella Romanelli, M., Sartiani, L., Masi, A., Mannaioni, G., Manetti, D., Mugelli, A., Cerbai, E., 2016. HCN channels modulators: the need for selectivity. Curr. Top. Med. Chem. 16, 1764–1791.
Pattnaik, B.R., Hughes, B.A., 2012. Effects of KCNQ channel modulators on the M-type potassium current in primate retinal pigment epithelium. Am. J. Physiol. Cell Physiol. 302, C821–C833.
Peng, L., Yang, C., Yin, J., Ge, M., Wang, S., Zhang, G., Zhang, Q., Xu, F., Dai, Z., Xie, L., Li, Y., Si, J.Q., Ma, K., 2019. TGF-Induces Gli1 in a Smad3-dependent manner against cerebral ischemia/reperfusion injury after isoflurane post-conditioning in rats. Front. Neurosci. 13, 636.
Qu, Y., Fang, M., Gao, B., Chui, R.W., Vargas, H.M., 2011. BeKm-1, a peptide inhibitor of human ether-a-go-go-related gene potassium currents, prolongs QTc intervals in isolated rabbit heart. J. Pharmacol. Exp. Therapeut. 337, 2–8.
Ramos-Mondragon, R., Galindo, C.A., Garcia-Castaneda, M., Sanchez-Vargas, J.L., Vega, A.V., Gomez-Viquez, N.L., Avila, G., 2012. Chronic potentiation of cardiac L-type Ca^{2+} channels by pirfenidone. Cardiovasc. Res. 96, 244–254.
Romanelli, M.N., Cerbai, E., Dei, S., Guandalini, L., Martelli, C., Martini, E., Scapecchi, S., Teodori, E., Mugelli, A., 2005. Design, synthesis and preliminary biological evaluation of zatebradine analogues as potential blockers of the hyperpolarization-activated current. Bioorg. Med. Chem. 13, 1211–1220.
Rosa, S.G.V., Santos, W.C., 2020. Clinical trials on drug repositioning for COVID-19 treatment. Rev. Panam. Salud Públic 44, e40.
Saito, S., Alkhatib, A., Kolls, J.K., Kondoh, Y., Lasky, J.A., 2019. Pharmacotherapy and adjunctive treatment for idiopathic pulmonary fibrosis (IPF). J. Thorac. Dis. 11, S1740–S1754.
Selyanko, A.A., Hadley, J.K., Wood, I.C., Abogadie, F.C., Delmas, P., Buckley, N.J., London, B., Brown, D.A., 1999. Two types of K^+ channel subunit, Erg1 and KCNQ2/3, contributes to the M-like current in a mammalian neuronal cell. J. Neurosci. 19, 7742–7756.
Simasko, S.M., Sankaranarayanan, S., 1997. Characterization of a hyperpolarization-activated cation current in rat pituitary cells. Am. J. Physiol. 272, E405–E414.
So, E.C., Foo, N.P., Ko, S.Y., Wu, S.N., 2019. Bisoprolol, known to be a selective β_1-receptor antagonist, differentially but directly suppresses $I_{K(M)}$ and $I_{K(erg)}$ in pituitary cells and hippocampal neurons. Int. J. Mol. Sci. 20, 657.
Stojilkovic, S.S., Bjelobaba, I., Zemkova, H., 2017. Ion channels of pituitary gonadotrophs and their roles in signaling and secretion. Front. Endocrinol. 8, 126.
Tanguay, J., Callahan, K.M., D'Avanzo, N., 2019. Characterization of drug binding within the HCN1 channel pore. Sci. Rep. 9, 465.
Togami, K., Kanehira, Y., Tada, H., 2015. Pharmacokinetic evaluation of tissue distribution of pirfenidone and its metabolites for idiopathic pulmonary fibrosis therapy. Biopharm Drug Dispos. 36, 205–215.
Van Bogaert, P.P., Pittoors, F., 2003. Use-dependent blockade of cardiac pacemaker current (If) by cilobradine and zatebradine. Eur. J. Pharmacol. 478, 161–171.
Wu, S.N., Chiang, H.T., Shen, A.Y., Lo, Y.K., 2003. Differential effects of quercetin, a natural polyphenolic flavonoid, on L-type calcium current in pituitary tumor (GH_3) cells and neuronal NG108-15 cells. J. Cell. Physiol. 195, 298–308.
Wu, S.N., Chern, J.H., Shen, S., Chen, H.H., Hsu, Y.T., Lee, C.C., Chan, M.H., Lai, M.C., Shie, F.S., 2017. Stimulatory actions of a novel thiourea derivative on large-conductance, calcium-activated potassium channels. J. Cell. Physiol. 232, 3409–3421.
Zhang, Y., Zhang, N., Gyulkhandanyan, A.V., Xu, E., Gaisano, H.Y., Wheeler, M.B., Wang, Q., 2008. Presence of functional hyperpolarisation-activated cyclic nucleotide-gated channels in clonal alpha cell lines and rat islet alpha cells. Diabetologia 51, 2290–2298.